Journal of Cluster Science (2022) 33:1667–1675
https://doi.org/10.1007/s10876-021-02090-9

ORIGINAL PAPER

Green Synthesis of Dense Rock MgO Nanoparticles Using *Carica Papaya* Leaf Extract and its Shape Dependent Antimicrobial Activity: Joint Experimental and DFT Investigation

Bhumika K. Sharma[1] · Bijal R. Mehta[1] · Vilas P. Chaudhari[1] · Esha V. Shah[1] · Sutapa Mondal Roy[2] · Debesh R. Roy[1]

Received: 30 March 2021 / Accepted: 11 May 2021 / Published online: 27 May 2021

Abstract

The present work reports the green synthesis of MgO nanoparticles (G-MgO NPs) using *Carica papaya* leaf extract, and a shape dependent density functional investigation for MgO NPs on their antimicrobial activity, for the first time. The synthesized G-MgO nanoparticles were characterized by *X*-ray diffraction (XRD), Fourier transform infrared spectroscopy (FT-IR), scanning electron microscopy (SEM) and Energy dispersive *X*-ray analysis (EDS). These methods confirmed the presence of the synthesized G-MgO nanoparticles in the range of 20–100 nm with the shape of dense rock. The larger particles of G-MgO NPs resulted from the agglomeration of smaller nanoparticles. The G-MgO NPs are observed to show reasonable antimicrobial activity against the microorganism *Bacillus subtilis.* A detailed theoretical study under density functional theory (DFT) shows that our synthesized dense rock shaped MgO nanoparticles are better candidate for biological interactions in comparison to the convensional spherical counterpart. The results show that the green synthesis of magnesium oxide nanoparticles using *Carica papaya* leaf extract can be an alternative to chemical and physical methods with possible biomedicinal applications in addition.

✉ Sutapa Mondal Roy
sutapa.roy@utu.ac.in

✉ Debesh R. Roy
drr@phy.svnit.ac.in

[1] Materials and Biophysics Group, Department of Physics, Sardar Vallabhbhai National Institute of Technology, Surat 395007, India

[2] Department of Chemistry, Uka Tarsadia University, Maliba Campus, Bardoli-Mahuva Road, Bardoli, Gujarat 394350, India

Graphic Abstract

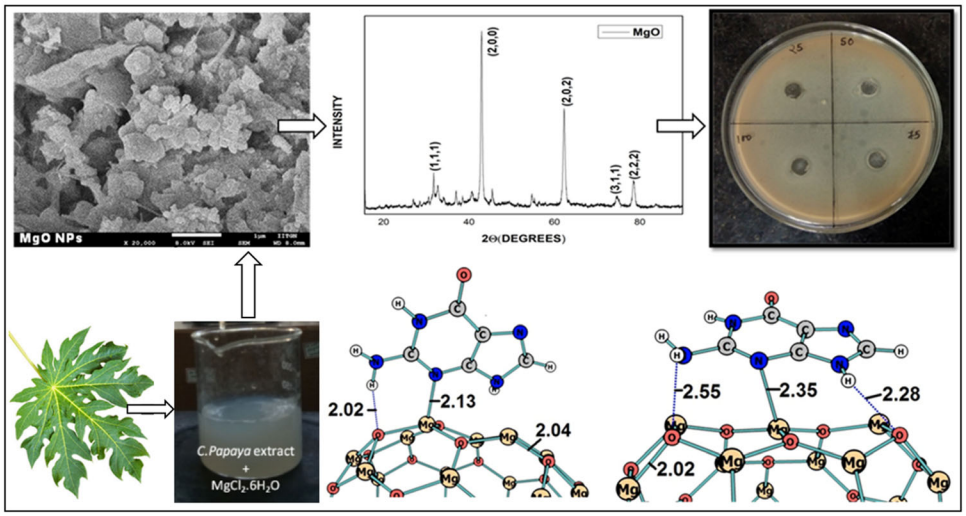

Keywords MgO nanoparticles · Green synthesis · *Carica papaya* · Antibacterial activity · Shape dependency · Density functional theory (DFT)

Introduction

Magnesium oxide is a very versatile compound due to its large abundance in the nature. Its rock salt crystal structure, thermodynamic stability, non conductive nature makes it more important compound for study [1]. Magnesium oxide (MgO) is most promising material due to its unique optical, mechanical, chemical, electrical properties and very high melting point and low heat capacity makes it excellent choice for insulation application. MgO at nanoscale shows very high reactivity because of the presence of high reactive edges and its high surface to volume ratio [2]. MgO is particularly distinguished by its favorable properties like flame resistance, dielectric resistance, and mechanical strength. MgO has numerous applications in various fields such as catalyst support, agriculture support, paint, and semiconductor, electro-optical devices, sensors, adsorption [2–8]. Mn/MgO was also utilized as a catalytic template for the growth of graphitic mesoporous carbon (GMC) [9]. Magnesium oxide nanoparticles can be synthesized by many physical and chemical routes such as sol–gel process, thermal decomposition, chemical precipitation, microwave-based method etc. [7, 8, 10].

Nanoparticles (NPs) synthesis by green methods are eco-friendly with low toxicity and they exhibit high stability [11]. MgO NPs are used as catalyst, electrochemical biosensors in pharmaceuticals industries and paint [12–15]. The nanoparticles synthesized using biological methods are simple and quick as compared to chemical and physical method. The beneficial role of leaf extract to be used as the reducing agent in the green synthesis process is that, unlike chemical reducing agents, use of leaf extract doesn't require any high temperature processing or any relevant toxic chemicals [16–18]. Further, green synthesis method has an advantage of cost effectiveness and can be used for the large-scale production of environment friendly nanoparticles [16–18]. MgO NPs have been synthesized using plants extract such as *Acacia gum* (AC) for the absorption of divalent metallic ions from synthetic wastewater [19]. *Clitoria ternatea* showing good antioxidant activity by DPPH activity, *Nephelium lappaceum* L peels, ethanolic fruit extract of *Emblica officinalis* showing antibacterial activity [20–22], etc. Many researchers have reported good antibacterial activity of MgO NPs which makes them important to study with different plant extract, microorganism and fungi.

In the present work, we have used *Carica papaya* leaf extract to prepare the nanoparticles (green synthesized MgO nanoparticles or G-MgO NPs) and to study the effect of nanoparticles on bacteria (antibacterial activity of G-MgO NPs). *Carica papaya*, belongs to the family of Caricaceae, and several species of Caricaceae have been used as a remedy against various diseases [23, 24]. The main constituent of *Carica papaya*, are papain, chymopapain, cystatin, à-tocopherol, ascorbic acid, flavonoids, cyanogenic glucosides, and glucosinolates which helps in regulating antioxidant power in the blood [25]. Magnesium oxide nanoparticles have good antibacterial activity against

Gram-negative and Gram-positive bacteria [21]. The supporting characterization and antibacterial activity are performed to show the shape size and morphology of synthesized nanoparticles.

Materials and Method

Analytical grade $MgCl_2.6H_2O$ was purchased from SRL, India. Deionized water (DI) water was used for the experiments. *Carica papaya* leaf extract was used as the reducing agent for the experiments.

Plant Extract

Carica papaya leaves were collected from SVNIT campus, Surat (Gujarat). The leaves were washed thoroughly with tap water for removal of dirt and dust, then they were washed with de-ionized water and were pat dried. The leaves were then cut into pieces. The leaves were then boiled in DI water for 2 h until the mixture volume reduced to half. The extract was filtered and was collected and stored for further experiments.

Synthesis of Plant Mediated Magnesium Oxide Nanoparticles

$MgCl_2.6H_2O$ was added to 50 ml of DI water and was allowed to boil until the salt gets dissolved completely to give 0.5 M solution. 10 ml of plant extract was drop wise added to the solution. The solution was allowed to boil for 2 h until visible color change is observed. The solution is then collected and calcined at 400 °C in tube furnace for 2 h. The whitish grey powder was collected and stored for further characterization.

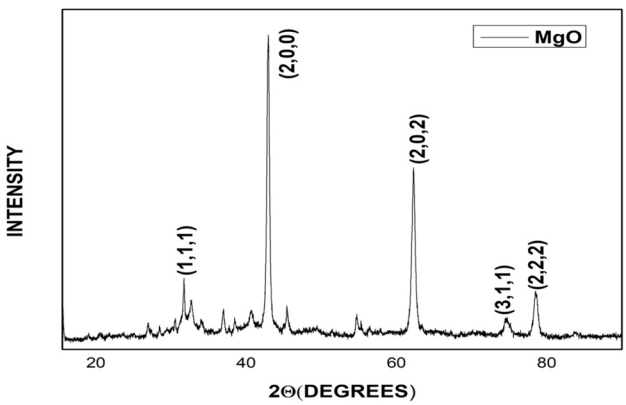

Fig. 1 XRD pattern of the green synthesized magnesium oxide nanoparticles

Theoretical Methods

One of the significant reasons in the study of clusters is to establish a fundamental understanding of materials from bulk to nanoscale dimension, as the properties and structures are often different, depending on the size and shape. Although it is important to study the interaction between nanoparticles and biomolecules, and their experimental observations, the current situation requires more detailed knowledge of the nanoparticle–biosystem interactions at the fundamental level. To understand the interactions between nanoparticles (MgO NPs) and biosystem (*Bacillus subtilis*), we have searched for the representative nanoclusters for MgO with spherical and rock shapes. For considerate of the experimental observation, the suitable nanoclusters with spherical and rock shapes of comparable average sizes, we have obtained spherical $(MgO)_{35}$ and rock $(MgO)_{36}$ nanoclusters of average measure about 1 nm for the investigation. On the other hand, we have considered the nuclic acids (DNA and RNA) base Guanine as the model biosystem for *B. subtilis*, since Guanine represents the maximum electronegativity compare to other nucleic acid bases Adenine, Cytosine, Thymine and Uracil [26]. Guanine's geometry and its complex with considered spherical and rock nanoclusters of $(MgO)_{35}$ and $(MgO)_{36}$, respectively are also optimized to gain more insight into their interactions. Here, in the present study, we have performed a detailed first-principles quantum chemical study of Guanine and its interaction with different MgO clusters. The optimized geometry of MgO clusters and Guanine interaction with MgO clusters were studied using a Density Functional Theory (DFT) [27] method by utilizing the Gaussian 09 [28] package program.

Results and Discussion

X-Ray Characterization

Crystal structure identification was made by X Ray Diffraction. The XRD pattern of G-MgO NPs prepared by green synthesis is shown in Fig. 1. The sharpness of the peaks shows that the particles are highly crystalline [11]. Figure 1 shows the formation of G-MgO NPs and the peaks matches very good as reported by Moorthy et al. [29] for G-MgO. The Scherrer's formula was used to calculate the crystallite sizes and was found to be in the range of 27 nm to 31 nm.

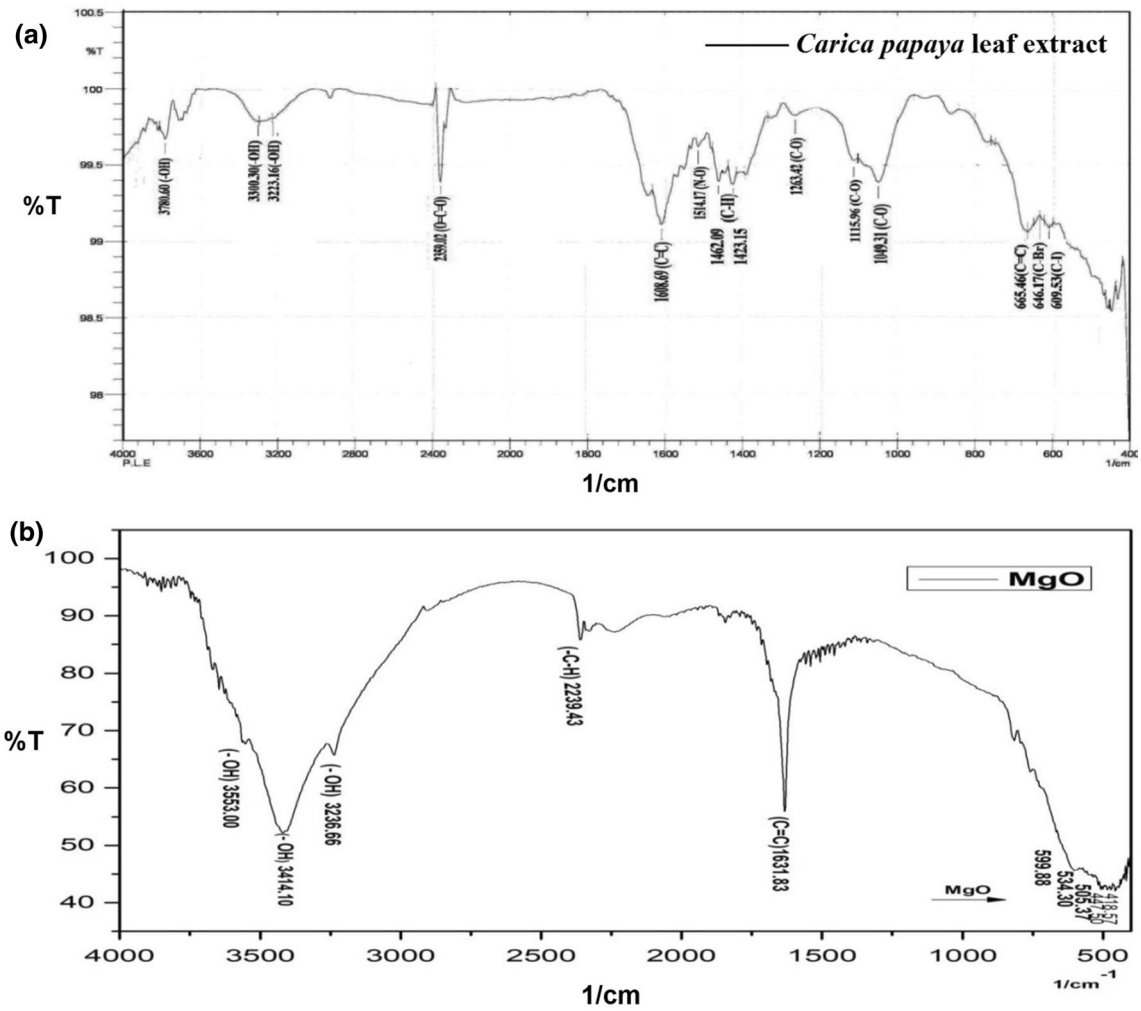

Fig. 2 FTIR spectra of (a) *Carica papaya* leaf extract and (b) G-MgO NPs using *Carica papaya* leaf extract

Fourier Transform Infrared Spectroscopy (FTIR)

The FTIR spectra of *Carica papaya* leaf extract is shown in Fig. 2a. The peaks represented in the spectrum (3780.60 cm^{-1}, 3300.33 cm^{-1} and 3223.16 cm^{-1}) are due to the –OH stretching, 2359.02 cm^{-1} is due to O = C = O stretching, 1608.69 cm^{-1} is due to > C = C < stretching of aromatic rings, 1514.17 cm^{-1} is for N–O stretching, 1462.02 cm^{-1} and 1423.51 cm^{-1} are for C–H stretching, 1263.42 cm^{-1} C–O for stretching of alkyl aryl ether, 1112.96 cm^{-1} and 1049.31 $cm^{-1}$for C–O stretching of alcohol group, 665.46 cm^{-1} for C = C bending of alkelene and 646.17 cm^{-1} and 609.53 cm^{-1} for C–Br and C–I stretching of halo groups respectively [30].

The FTIR spectra of G-MgO NPs by green synthesis using *Carica papaya* leaf extract, is shown in Fig. 2b. The peaks at 3553.00 cm^{-1}, 3414.10 cm^{-1}, and 3236.66 cm^{-1} corresponds to –OH stretching, the peaks at 2239.43 cm^{-1} and 1631.83 cm^{-1} were attributed to alkyl C–H stretching and alkenyl > C = C < stretching respectively. The presence of peaks at 500–300 cm^{-1} strongly confirms the stretching vibrations between metal and oxygen (Mg–O) [22].

Scanning Electron Spectroscopy and Energy Dispersive Spectroscopy (EDS)

Scanning electron microscopy of green synthesized G-MgO NPs are shown in Fig. 3. The surface morphology of G-MgO NPs showed relatively dense rock structure. It was also shown that the particles were found to be in the range of 20–100 nm. The aggregation of the nanoparticles over each other is due to the electrostatic interactions between the bioorganic capping molecules bound to the surface of the G-MgO NPs. The EDS study showed the purity of magnesium (Mg) and oxygen (O) attributed in the synthesized nanoparticles with the presence of carbon

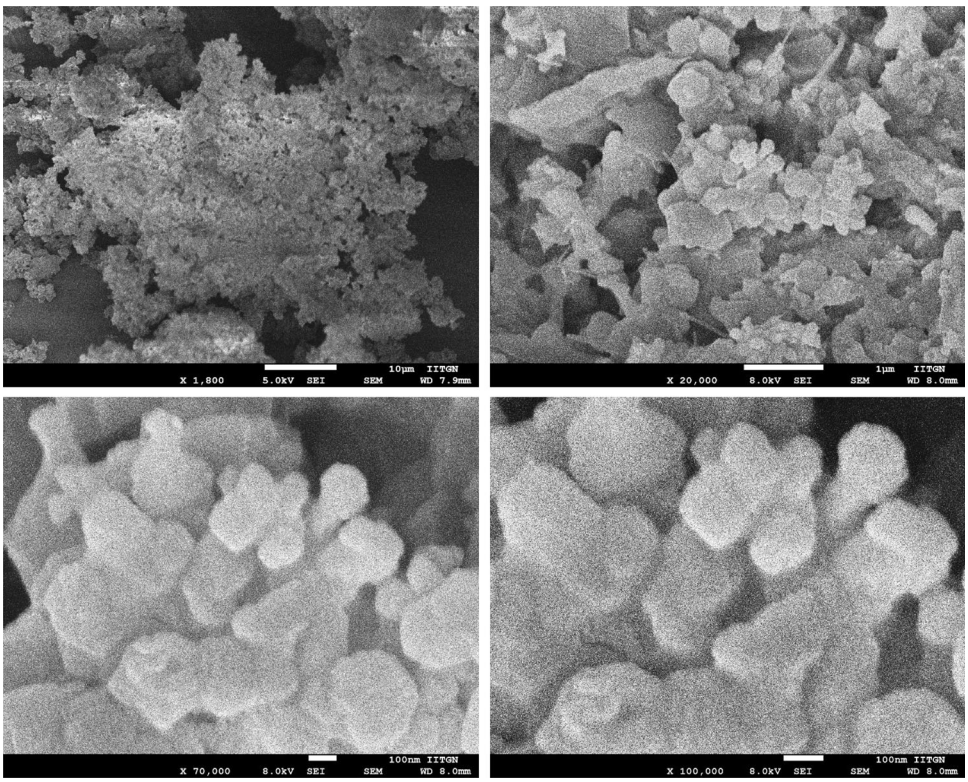

Fig. 3 SEM morphology of G-MgO NPs using *Carica papaya* leaf extract

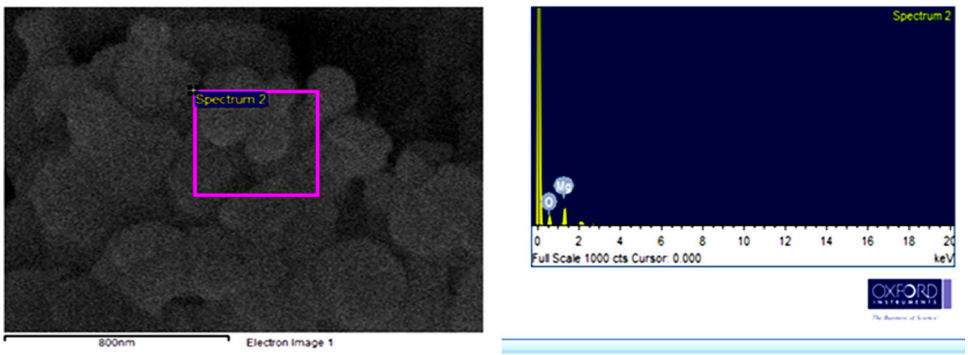

Fig. 4 EDAX of G-MgO NPs using *Carica papaya* leaf extracts

showing the capping of the plant extract used. The elemental mapping of these G-MgO NPs is shown in Fig. 4.

Antibacterial Activity

The antibacterial activity of MgO nanoparticles synthesized using *Carica papaya* leaf extract was studied by Agar cup method in terms of Zone of Inhibition (ZOI). A well of 8 mm diameter, i.e. borer diameter (B_d) was punched into Luria broth agar having the microorganisms. The minimum concentration of G-MgO NPs was 75 µl with zone of inhibition of 10 mm ± 0.25. The study was carried out on Gram-positive bacterial strain *Bacillus subtilis*. The clear zone indicates the growth inhibition of the bacteria which is shown in Fig. 5 due to the diffusion of nanoparticles. The results are tabulated in Table 1. Due to interaction between nanoparticles and microorganism, reduction in the growth of bacteria was observed. The zone of inhibition was observed on implication of nanoparticles with different concentration. Increase in the concentration of nanoparticles leads to the increase in zone of inhibition of the bacterial strain. The diffusion of the nanoparticles in the ionic form results in chemical reaction and deformation of DNA of the bacteria resulting in the cell toxicity [31]. It may be noted from the Table 1 that the increase of concentration of the MgO NPs in the considered range doesn't show significant difference in their antimicrobial activity against *B. subtilis*, and similar small effect is also reported for MgO NPs by Suresh et al. [21] in past, for other bacterial strains. However, the most important observation in all these cases is that the increase of MgO NPs concentration (in µL or

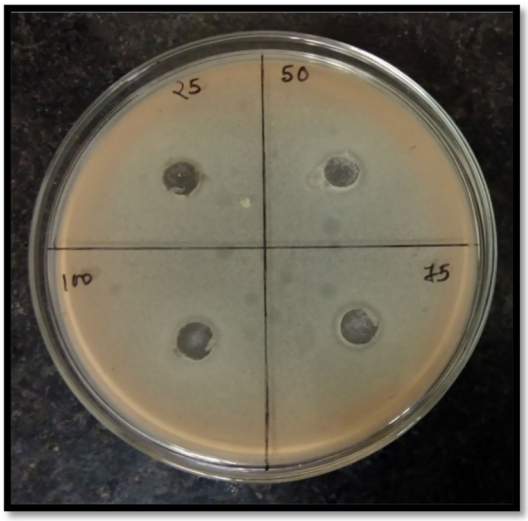

Fig. 5 Antibacterial activity of G-MgO NPs, synthesized using *Carica papaya* leaf extract on *Bacillus subtilis*

mg/mL [21]) leads to the increase in antibacterial effect (8.5 to 10.1 mm for *B. subtilis*, in present work; 8.0 to 11.0 mm for *E. coli* [21] and 5.0 to 6.0 mm for *R. solanacearum* [21]). These observations suggest the slow and systematic increase in antibacterial activity of MgO NPs, which may be a general characteristic of these nanoparticles with possible medicinal applications.

Due to the small size of synthesized G-MgO NPs, they provide larger surface to volume ratio and its spherical shape makes it easier to interact with microorganisms, which is clearly observed in Table 1. It may be noted that in present work MgO NPs ranging from 20–100 nm, in spherical shape shows significant antimicrobial activity with considered nanoparticles concentrations ranging from 50 µl to 100 µl. In past, many researchers have studied different MgO NPs with different physical, chemical and green methods of synthesis, and studied their antibacterial activities [11, 32–35] in which some of the important literatures are tabulated in Table 2. For a comparison of the ZOI′ for our synthesized G-MgO NPs against *B. subtlits* at 50 µl is also reported (9.0 mm) in the table. It may be noted that our synthesized MgO with *Carica papaya* leaf extracts shows similar antimicrobial activity with the same concentration of nanoparticles of other reported green and/or chemical and physical methods. Overall, the results of the present work indicate that the novel use of *Carica papaya* leaf extracts for synthesis of magnesium oxide nanoparticles may be a better alternative to physical and chemical methods, and also for the biomedicinal aspects of G-MgO NPs.

Table 1 Antibacterial activity of G-MgO NPs evaluated in terms of Zone of inhibition (ZOI, mm) against *B. subtlities* at different concentration (in µl)

Bacteria	Concentration of G-MgO NPs (µl)	ZOI′ (incl. B_d) (mm)	ZOI = ZOI′-B_d (mm)
B. subtlities	25 µl	08.5 ± 0.25	0.5 ± 0.25
	50 µl	09.0 ± 0.25	1.0 ± 0.25
	75 µl	10.0 ± 0.25	2.0 ± 0.25
	100 µl	10.1 ± 0.25	2.1 ± 0.25

Table 2 Antibacterial activities, of some MgO nanoparticles prepared through chemical, physical and green synthetic methods, in terms of size of the nanoparticles and ZOI

Sl	Synthesis	Methods	Size (nm) (Shape)	NPs conc	ZOI′ (mm)	Organisms	Ref's
1	Physical	Microwave hydrothermal	6–8 (Nanowire)	50 µl	12.2	*B. subtlits*	[32]
2	Chemical	Precipitation-calcination method	27, 32 (flakes)	0.5 mg	8.6	*S. aureus*	[33]
3	Green	Betel leaf	∼ 18	60 µg	20.0	*B. subtlits*	[11]
4	Green	Aloe Vera	140 (Spherical)	25 µl	4.6	*S. aureus*	[34]
5	Green	Ocimum sanctum	50–100 (dense flakes)	100 µl	14.0	*S. aureus*	[35]
6	Green	Carica papaya leaf	20–100 (dense rock)	50 µl	9.0	*B. subtlits*	Present work

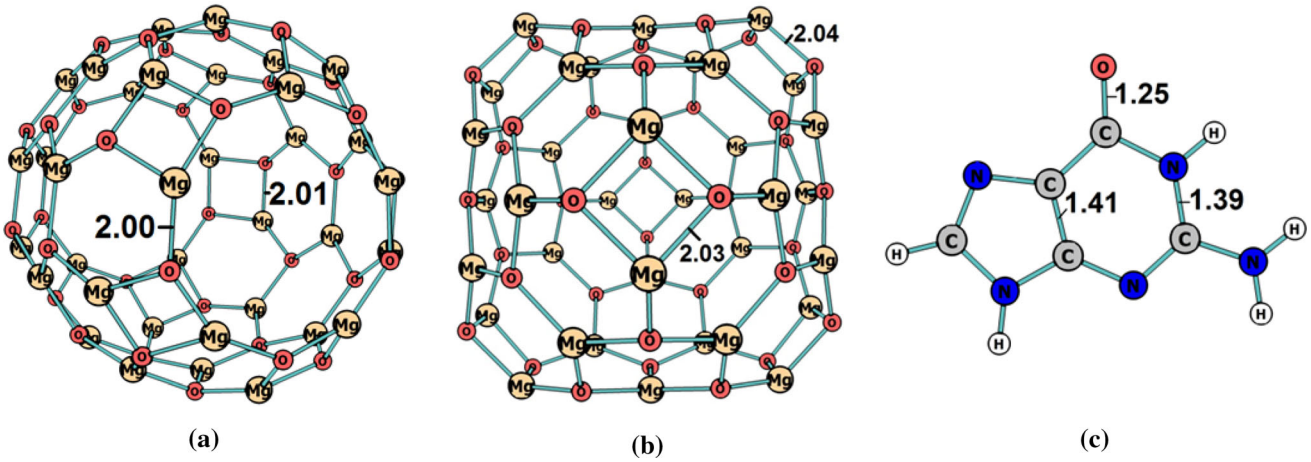

Fig. 6 The optimized geometries of (a) $(MgO)_{35}$ (spherical), (b) $(MgO)_{36}$ (rock) nanoclusters and (c) Guanine nucleic acid base

Table 3 Chemical hardness (η), electronegativity (χ), electrophilicity index (ω), electron transfer (ΔN) and energy transfer (ΔE) with Guanine for the modeled $(MgO)_{35}$ (spherical) and $(MgO)_{36}$ (rock) magnesium oxide nanoparticles

Systems	η (e*V*)	χ (e*V*)	ω (e*V*)	ΔN (e*V*)	ΔE (e*V*)
Guanine	2.67	3.33	2.08	–	–
$(MgO)_{35}$: Spherical	2.53	3.64	2.62	0.030	0.005
$(MgO)_{36}$: Rock	2.39	3.74	2.93	0.040	0.008

Theoretical

We have accomplished a detailed calculation on the comparative shape dependent bio-activities for spherical and rock shaped MgO NPs against a biological target like *Bacillus subtilis*. The spherical $(MgO)_{35}$ and rock $(MgO)_{36}$ nanoclusters of average size of about 1 nm are considered as the representatives for individual nanoparticle. As a well-accepted fact that a nanoparticle is expected to interact well with nucleic acids (DNA and RNA) bases in a biosystem, we have chosen the highest electronegative nucleic acid base Guanine [26] as the model biosystem for *B. subtilis*.

Figure 6 presents the optimized geometries of spherical $(MgO)_{35}$ and rock $(MgO)_{36}$ nanoclusters, and the Guanine nucleic acid base. The representative spherical and rock MgO nanoclusters are considered with a comparable average size of about 1 nm to meet the property of a representative nanoparticle's in order to understand our experimental observations.

Table 3 represents the chemical hardness [27], electronegativity [27] and electrophilicity index [36, 37] values of Guanine, $(MgO)_{35}$ and $(MgO)_{36}$. The electron and energy transfer values of spherical $(MgO)_{35}$ and rock shaped $(MgO)_{36}$ nanoclusters with model biosystem Guanine is also reported. The higher electrophilicity value of rock $(MgO)_{36}$ (2.93 eV) in comparison to its spherical counterpart indicate its more reactive nature, which may facilitate better interaction to the biosystem. Also, more electron transfer (ΔN) and energy transfer (ΔE) of rock

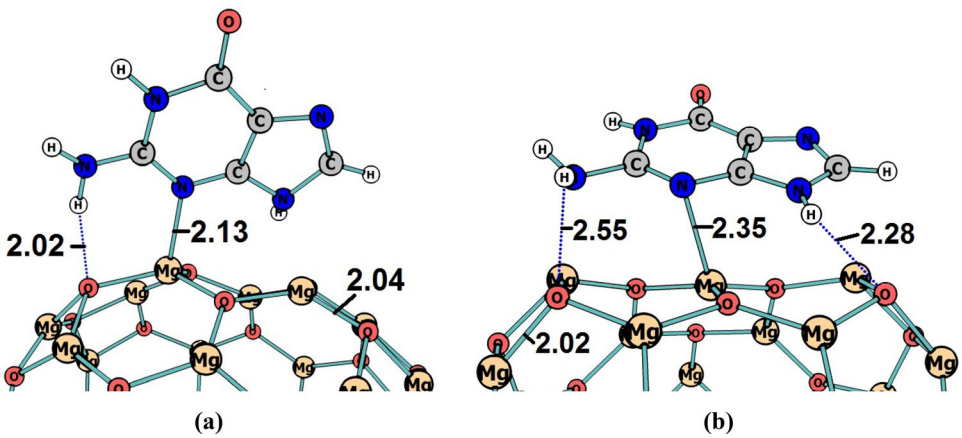

Fig. 7 The optimized geometries of (a) $(MgO)_{35}$ (spherical)–Guanine and (b) $(MgO)_{36}$ (rock)–Guanine interactions

$(MgO)_{36}$ with model biosystem Guanine confirms its potency over the spherical particle for better biological activity facilitated with larger electronic interactions.

A large-scale simulation was performed to investigate the exact interaction of the considered spherical and rock nanoclusters with Guanine. The optimized structures of spherical $(MgO)_{35}$-Guanine and rock $(MgO)_{36}$-Guanine is shown in Fig. 7. It may be noted from the figure that Guanine shows stronger adsorption on the surface of rock nanocluster (Fig. 7b) with two hydrogen bond interactions (O….H) over its spherical counterpart (single O···H bond, Fig. 7a). The present theoretical study indicates that the dense rock MgO nanoparticles, as observed in our present experiment, are more reactive and biologically active compared to prototypical spherical MgO nanoparticles.

Concluding Remarks

In summary, present study address the green synthesis, characterizations and antimicrobial activities of MgO nanoparticles (G-MgO NPs) using *Carica papaya* leaf extract. The *X*-ray diffraction (XRD) analysis shows good crystallinity of the NPs with the calculated particle size between 27 and 31 nm. Fourier transform infrared spectroscopy (FT-IR) confirms the attachment of functional groups and capping agent, and bands located near 500–300 cm $^{-1}$ strongly confirms the formation of G-MgO NPs. Scanning electron microscopy (SEM) and Energy dispersive *X*-ray analysis (EDS) confirmed the presence of the synthesized G-MgO NPs in the range of 20–100 nm with the shape of dense rock. The dense rock shaped G-MgO NPs are observed to show reasonable antibacterial activity against the microorganism *Bacillus subtilis*. Our theoretical investigations confirm that our synthesized dense rock shaped G-MgO NPs are better candidate for biological activity in comparison to its conventional spherical counterpart. Overall, the results indicate that the green synthesis of dense rock magnesium oxide nanoparticles using *Carica papaya* leaf extract can be a better alternative to chemical and physical methods, along with its added advantage for possible biomedicinal applications.

Acknowledgements DRR is thankful to the SERB, New Delhi, Govt. of India for financial support (Grant No. CRG/2020/002634). BKS is thankful for her UGC-RGNF fellowship (RGNF-2017-18-SC-GUJ-35487).

Declarations

Conflict of interest The authors declare that they have no conflict of interest.

References

1. S. Stankic, M. Müller, O. Diwald, M. Sterrer, E. Knözinger, and J. Bernardi (2005). Size-dependent optical properties of MgO nanocubes. *Angewandte Chemie International Edition* **44** (31), 4917–4920.
2. A. Fakhri and S. Adami (2014). Adsorption and thermodynamic study of Cephalosporins antibiotics from aqueous solution onto MgO nanoparticles. *Journal of the Taiwan Institute of Chemical Engineers* **45** (3), 1001–1006.
3. A. B. Patil and B. M. Bhanage (2013). Novel and green approach for the nanocrystalline magnesium oxide synthesis and its catalytic performance in Claisen-Schmidt condensation. *Catalysis Communications* **36**, 79–83.
4. B. Nagappa and G. T. Chandrappa (2007). Mesoporous nanocrystalline magnesium oxide for environmental remediation. *Microporous and Mesoporous Materials* **106** (1–3), 212–218.
5. R. Al-Gaashani, S. Radiman, Y. Al-Douri, N. Tabet, and A. R. Daud (2012). Investigation of the optical properties of Mg (OH) 2 and MgO nanostructures obtained by microwave-assisted methods. *Journal of Alloys and Compounds* **521**, 71–76.
6. F. Mohandes, F. Davar, and M. Salavati-Niasari (2010). Magnesium oxide nanocrystals via thermal decomposition of magnesium oxalate. *Journal of Physics and Chemistry of Solids* **71** (12), 1623–1628.
7. P. Ouraipryvan, T. Sreethawong, and S. Chavadej (2009). Synthesis of crystalline MgO nanoparticle with mesoporous-assembled structure via a surfactant-modified sol–gel process. *Mater. Lett.* **63**, 1862–1865.
8. W. Wang, X. Qiao, J. Chen, and H. Li (2007). Facile synthesis of magnesium oxide nanoplates via chemical precipitation. *Materials Letters* **61** (14–15), 3218–3220.
9. R. Atchudan, S. Perumal, D. Karthikeyan, A. Pandurangan, and Y. R. Lee (2015). Synthesis and characterization of graphitic mesoporous carbon using metalemetal oxide by chemical vapor deposition method. *Microporous and Mesoporous Materials* **215**, 123–132.
10. K. D. Bhatte, D. N. Sawant, K. M. Deshmukh, and B. M. Bhanage (2012). Additive free microwave assisted synthesis of nanocrystalline Mg (OH) 2 and MgO. *Particuology* **10** (3), 384–387.
11. G. Palanisamy and T. Pazhanivel (2017). Green synthesis of MgO nanoparticles for antibacterial activity. *Int Res J Eng and Technol* **4** (9), 137–141.
12. H. Tsuji, F. Yagi, H. Hattori, and H. Kita (1994). Self-condensation of n-butyraldehyde over solid base catalysts. *Journal of Catalysis* **148** (2), 759–770.
13. Lu, L., Zhang, L., Zhang, X., Wu, Z., Huan, S., Shen, G. and Yu, R., 2010. A MgO Nanoparticles Composite Matrix-Based Electrochemical Biosensor for Hydrogen Peroxide with High Sensitivity. *Electroanalysis: An International Journal Devoted to Fundamental and Practical Aspects of Electroanalysis*, *22*(4), pp.471–477.
14. S. Shen, P. S. Chow, F. Chen, and R. B. H. Tan (2007). Submicron particles of SBA-15 modified with MgO as carriers for controlled drug delivery. *Chemical and pharmaceutical bulletin* **55** (7), 985–991.
15. P. Yang and C. M. Lieber (1996). Nanorod-superconductor composites: a pathway to materials with high critical current densities. *Science* **273** (5283), 1836–1840.
16. P. C. Nagajyothi, P. Muthuraman, T. V. M. Sreekanth, D. H. Kim, and J. Shim (2016). Green synthesis: In-vitro anticancer activity of copper oxide nanoparticles against human cervical carcinoma cells. *Arabian Journal of Chemistry* **10**, 215–225.

17. A. K. Mittal, Y. Chisti, and U. C. Banerjee (2013). Synthesis of metallic nanoparticles using plant extracts. *Biotechnology advances* **31** (2), 346–356.
18. B. K. Sharma, D. V. Shah, and D. R. Roy (2018). Green synthesis of CuO nanoparticles using Azadirachta indica and its antibacterial activity for medicinal applications. *Mater. Res. Express* **5**, 095033.
19. V. Srivastava, Y. C. Sharma, and M. Sillanpää (2015). Green synthesis of magnesium oxide nanoflower and its application for the removal of divalent metallic species from synthetic wastewater. *Ceramics International* **41** (5), 6702–6709.
20. N. J. Sushma, D. Prathyusha, G. Swathi, T. Madhavi, B. D. P. Raju, K. Mallikarjuna, and H. S. Kim (2016). Facile approach to synthesize magnesium oxide nanoparticles by using Clitoria ternatea—characterization and in vitro antioxidant studies. *Applied Nanoscience* **6** (3), 437–444.
21. Suresh, J., Yuvak kumar, R., Sundrarajan, M. and Hong, S.I., 2014. Green synthesis of magnesium oxide nanoparticles. In *Advanced Materials Research* (Vol. 952, pp. 141–144). Trans Tech Publications.
22. K. Ramanujam and M. Sundrarajan (2014). Antibacterial effects of biosynthesized MgO nanoparticles using ethanolic fruit extract of Emblica officinalis. *Journal of photochemistry and photobiology B: biology* **141**, 296–300.
23. V. J. Mello, M. T. R. Gomes, F. O. Lemos, J. L. Delfino, S. P. Andrade, M. T. Lopes, and C. E. Salas (2008). The gastric ulcer protective and healing role of cysteine proteinases from Carica candamarcensis. *Phytomedicine* **15** (4), 237–244.
24. Munoz, V., Sauvain, M., Bourdy, G., Callapa, J., Rojas, I., Vargas, L., Tae, A. and Deharo, E., 2000. The search for natural bioactive compounds through a multidisciplinary approach in Bolivia. Part II. Antimalarial activity of some plants used by Mosetene indians. *Journal of ethnopharmacology*, *69*(2), pp.139–155.
25. D. S. Seigler, G. F. Pauli, A. Nahrstedt, and R. Leen (2002). Cyanogenic allosides and glucosides from Passiflora edulis and Carica papaya. *Phytochemistry* **60** (8), 873–882.
26. Mondal Roy, S. and Roy, D. R. 2019. Modeling of Bio-Activity and Toxicity in Light of NA Bases Interaction, Scholars' Press, Latvia: European Union.
27. R. G. Parr and W. Yang, *Density functional Theory of Atoms and Molecules* (Oxford University Press, New York, USA, 1989).
28. Frisch, M.J. et al., GAUSSIAN 09, Revision D.01; Gaussian, Inc., Pittsburgh PA, USA, 2009.
29. S. K. Moorthy, C. H. Ashok, K. V. Rao, and C. Viswanathan (2015). Synthesis and characterization of MgO nanoparticles by Neem leaves through green method. *Materials Today: Proceedings* **2** (9), 4360–4368.
30. Fadare, O.A., Durosinmi, O.M., Fadare, R., Izevbekhai, O.U., Awonyemi, I.O. and Obafemi, C.A., 2015. ATR-FTIR and HPLC spectroscopic studies and evaluation of mineral content of Carica papaya leaves and flowers.
31. A. Azam, A. S. Ahmed, M. Oves, M. S. Khan, S. S. Habib, and A. Memic (2012). Antimicrobial activity of metal oxide nanoparticles against Gram-positive and Gram-negative bacteria: a comparative study. *International journal of nanomedicine* **7**, 6003.
32. F. Al-Hazmi, F. Alnowaiser, A. A. Al-Ghamdi, A. A. Al-Ghamdi, M. M. Aly, R. M. Al-Tuwirqi, and F. El-Tantawy (2012). A new large–scale synthesis of magnesium oxide nanowires: structural and antibacterial properties. *Superlattices and Microstructures* **52** (2), 200–209.
33. B. Vatsha, P. Tetyana, P. M. Shumbula, J. C. Ngila, L. M. Sikhwivhilu, and R. M. Moutloali (2013). Effects of precipitation temperature on nanoparticle surface area and antibacterial behaviour of Mg (OH) 2 and MgO nanoparticles. *Journal of Biomaterials and Nanobiotechnology* **4** (04), 365.
34. Soma Prabha A. and Praba karan V. 2017 Green synthesis of magnesium oxide as nanoparticle synthesis from plant extract and its biological activity. Soma Prabha A and Praba karan V *International Journal of Current Advanced Research Vol 6, Issue 09, pp 5826-5832.*
35. T. Sobana Premlatha and M. Preethika (2018). Synthesis and characterisation of magnesium oxide nanoparticles using ocimum sanctum and its application. *World Journal of Pharmaceutical Research* **7** (7), 285–294.
36. Chattaraj, P. K. and Roy, D. R. 2007. Update 1 of: Electrophilicity index. *Chem. Rev.*, 107, pp.PR46-PR74.
37. P. K. Chattaraj, U. Sarkar, D. R. Roy, M. Elango, R. Parthasarathi, and V. Subramanian (2006). Is electrophilicity a kinetic or a thermodynamic concept? *Ind. J. Chem. A* **45A**, 1099–1112.